NASA TECHNICAL NOTE

NASA TN D-5892
C. 1

LOAN COPY: RETURN
AFWL (WLOL)
KIRTLAND AFB. N M

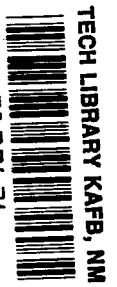

NASA TN D-5892

HIGH TEMPERATURE EQUATION OF STATE FOR ALUMINUM

by R. J. Naumann

George C. Marshall Space Flight Center
Marshall Space Flight Center, Ala. 35812

NATIONAL AERONAUTICS AND SPACE ADMINISTRATION • WASHINGTON, D. C. • AUGUST 1970

TECH LIBRARY KAFB, NM
0132626

TECHNICAL RE.

1. REPORT NO. NASA TN D-5892	2. GOVERNMENT ACCESSION NO.	3. RECIPIENT'S CATALOG NO.
4. TITLE AND SUBTITLE High Temperature Equation of State for Aluminum		5. REPORT DATE August 1970 6. PERFORMING ORGANIZATION CODE
7. AUTHOR(S) R. J. Naumann		8. PERFORMING ORGANIZATION REPORT #
9. PERFORMING ORGANIZATION NAME AND ADDRESS George C. Marshall Space Flight Center Marshall Space Flight Center, Alabama 35812		10. WORK UNIT NO. 11. CONTRACT OR GRANT NO.
12. SPONSORING AGENCY NAME AND ADDRESS		13. TYPE OF REPORT & PERIOD COVERED Technical Note 14. SPONSORING AGENCY CODE

15. SUPPLEMENTARY NOTES

Prepared by Space Sciences Laboratory,
Science and Engineering Directorate.

16. ABSTRACT

An equation of state is developed for metallic elements that describes both the solid and liquid phase at very high temperatures and pressures. Computations are carried out for aluminum which are compared with experimental results obtained from shocking porus samples.

17. KEY WORDS	18. DISTRIBUTION STATEMENT Distribution Categories 1 12 17 18 23

19. SECURITY CLASSIF. (of this report)	20. SECURITY CLASSIF. (of this page)	21. NO. OF PAGES	22. PRICE *
Unclassified	Unclassified	21	$3.00

*For sale by the Clearinghouse for Federal Scientific and Technical Information
Springfield, Virginia 22151

TABLE OF CONTENTS

LIST OF TABLES

LIST OF ILLUSTRATIONS

HIGH TEMPERATURE EQUATION OF STATE FOR ALUMINUM [1]

By

R. J. Naumann

SUMMARY

An equation of state is developed that is capable of describing metallic elements in both solid and liquid phase from ambient temperature and pressures to states of extreme temperature and pressure. A novel technique for treating the atomic vibrational contributions is introduced by assuming each atom vibrates independently in a $\tan^2$ potential. The Schroedinger equation can be solved exactly for this potential function, and the quantum mechanical partition function is computed directly. In this manner a continuous, thermodynamically consistent description of metals is obtained which reduces to an Einstein solid at moderate temperatures and to an ideal gas in the limits of high temperatures and/or large volumes.

Detailed numerical computations are carried out for aluminum. All the constants required to configure the model are obtainable from elementary thermodynamic data at ambient conditions. Excellent agreement is obtained with experimental shock compression data on solid and porous samples at pressures to 5 Mb and temperatures to 25 000°K.

INTRODUCTION

Substantial progress has been made in recent years in understanding the behavior of metals at extreme temperatures and pressures. Shock compression techniques have achieved pressure measurements to approximately 10 Mb and temperatures of tens of thousands degrees [1]. At the lower pressures, the Debye or Einstein model for energy and the Mie-Gruneisen equation for pressure is adequate and zero-degree isotherms were extracted from shock measurements by using these relations to subtract out the thermal contributions. It was found that a Morse potential predicted the zero-degree isotherms to a fair degree of accuracy [2], which confirmed an earlier suggestion by Slater [3].

As experimental pressures and temperatures increased, various inadequacies in the theory became evident. Electronic contributions were introduced. For compressible metals, anharmonic terms became significant. These were treated by Al'tshuler et al. using the free volume theory of Lennard-Jones and Devonshire [4]. Pastine [5] used the perturbation method of Liebfried and Ludwig [6] to correct for anharmonic effects.

For the high-temperature states reached by shocking porous samples, it was found that the behavior became more ideal gas-like. Kormer [7] proposes a set of empirical interpolation equations to transform solid-like behavior of energy, pressure, and heat capacity to the ideal gas relations. Urlin [8] proposed an empirical free energy function to account for phase transitions. All of these empirical relations require adjustable constants which are evaluated from experimental high-pressure data. Furthermore, there is no guarantee of thermodynamic consistency between them[2].

An equation of state for metals is developed in this work that is capable of describing the liquid-dense vapor phase as well as the solid phase from ambient conditions to temperatures and pressures exceeding the present experimental range. Rather than use interpolation equations to transform the behavior of a solid to that of a gas at high temperatures or at low densities, the approach will be to start with empirical interatomic potential functions and develop the entire equation of state using quantum statistical mechanics. The only empirical constants required are obtainable from elementary thermodynamic quantities such as

---

1. This report was based on work submitted in partial fulfillment of the requirements for the degree of Doctor of Philosophy in the Department of Physics in the Graduate School of the University of Alabama.

2. Kormer's pressure, energy, and heat capacity were chosen in such a manner to be consistent among themselves.

heat of vaporization, compressibility, entropy, etc. In this manner the behavior of a metal throughout the entire high-pressure, high-temperature regime can be predicted from its properties at ambient conditions. Since all the thermodynamic properties are derived from the partial function, thermodynamic consistency is guaranteed. This allows a complete thermodynamic description , so that phase transitions are described naturally from Gibbs energy considerations.

FORMULATION

It will be assumed that the Helmholtz energy can be expressed as the sum of three independent contributions: the lattice term, F_k, the ionic vibration term, F_v, and the free electronic term, F_e. Since all thermodynamic functions are derivable from the Helmholtz energy, it immediately follows that they all can be expressed as sums of these three contributions. The fact that there are interactions between the free electrons and the lattice will be accounted for by introducing an effective electron mass.

Lattice Terms

Since the Morse potential has been found to be a reasonable empirical representation for the lattice energy of a metallic solid, the Helmholtz energy for the zero-degree lattice is written

$$F_k = L_o \left(e^{2b(1-\xi)} - 2e^{b(1-\xi)} \right) \quad , \qquad (1)$$

where L_o is the zero-degree heat of vaporization, or total binding energy, $\xi = (V/V_o)^{1/3}$, and b is an empirical constant determined from the compressibility. From the relation $F = E - TS$, the internal energy, E_k, of the zero-degree lattice is identical to F_k. The zero-degree isotherm is found from the relation

$$P = - (\partial F_k/\partial V)_T$$

and is

$$P_k = \frac{2L_o b}{3V_o \xi^2} \left(e^{2b(1-\xi)} - e^{b(1-\xi)} \right) \qquad (2)$$

Vibrational Terms

At moderate temperatures, the ionic vibrational contributions may be computed from the assumption that the ions behave as harmonic oscillators. This assumption leads to the Einstein model, in which it is assumed that all atoms vibrate independently at the same frequency, or to the Debye model which considers a distribution of normal mode frequencies. At very high temperatures, the vibrational amplitudes are such that nonlinear restoring forces must be considered. This is accounted for by assuming each atom vibrates independently[3] in a potential well given by

$$\Phi(x) = \frac{2a^2 m\omega_E^2}{\pi^2} \tan^2 \left(\frac{\pi x}{2a} \right) \quad . \qquad (3)$$

When the displacement x is small compared to the atomic spacing a, the potential reduces to

$$\Phi(x) = \frac{m\omega_E^2}{2} x^2 \quad , \qquad (4)$$

where ω_E is the Einstein frequency. For a harmonic oscillator, $\omega^2 = K/m$, therefore, equation (4) has the form $1/2\ Kx^2$ where K is the spring constant corresponding to the Einstein frequency.

At larger displacements, $x \approx \pm a$, the potential approaches infinity which describes a hard sphere collision between point masses. This roughly corresponds to nuclear collisions between neighboring atoms whose position expectation values are $\pm a$.

The choice of the $\tan^2$ functional representation was made because it behaves as desired in the limits

3. The assumption of independent vibration is justified because even at moderate temperatures the Einstein and Debye models give almost identical results.

and also because it allows a closed-form-eigenvalue solution to the Schroedinger equation. The energy eigenvalues are[4]

$$\epsilon_n = (n^2 + n)\,\epsilon_o + n\left(\hbar^2\omega_E^2 + \epsilon_o^2\right)^{1/2} \quad , \qquad n = 0, 1, 2, \ldots \tag{5}$$

where ϵ_o is the degeneracy energy $\pi^2\hbar^2 / (8\ m\ a^2)$.

The vibrational partition function Z for N atoms, each with three degrees of freedom, is

$$\ln Z = 3N \ln \sum_{n=0}^{\infty} e^{-\epsilon_n/kT} \tag{6}$$

where k is the Boltzmann constant.

The various thermodynamic functions are obtained from the partition function in the usual manner.

$$F_v = -kT \ln Z = -3NkT \ln \sum_{n=0}^{\infty} e^{-\epsilon_n/kT} , \tag{7}$$

$$E_v = kT^2 \frac{\partial \ln Z}{\partial T} = 3N \left\langle \epsilon_n \right\rangle , \tag{8}$$

$$C_{vv} = \left(\frac{\partial E_v}{\partial T}\right)_V = \frac{3N}{kT^2}\left[\left\langle \epsilon_n^2 \right\rangle - \left\langle \epsilon_n \right\rangle^2\right] , \tag{9}$$

and

$$P_v = -kT \frac{\partial}{\partial V} \ln Z = 3N \left\langle P_n \right\rangle , \tag{10}$$

where

$$P_n = -\frac{\partial \epsilon_n}{\partial V} \tag{11}$$

Differentiating equation (5), the P_n contribution becomes

$$P_n = (n^2+n)\frac{2}{3}\frac{\epsilon_o}{V} + \frac{n}{V}\left[\frac{\gamma\hbar^2\omega^2 + \frac{2}{3}\epsilon_o^2}{(\hbar^2\omega^2 + \epsilon_o^2)^{1/2}}\right] , \tag{12}$$

where γ is the Gruneisen ratio, $-(\partial \ln \omega / \partial \ln V)$. Formulation of γ for solids has received extensive treatment in the literature.

The brackets $\langle\ \rangle$ denote the ensemble average; eg.,

$$\left\langle x \right\rangle = \frac{\sum_{n=0}^{\infty} x\, e^{-\epsilon_n/kT}}{\sum_{n=0}^{\infty} e^{-\epsilon_n/kT}} . \tag{13}$$

At solid densities, $\hbar\omega >> \epsilon_o$ and the Boltzmann factor reduces to $\exp\left[-(n^2\epsilon_o + n\hbar\omega)/kT\right]$. Unless $kT >> \hbar\omega$, the Boltzmann factor will become negligibly small at low enough values of n to prevent the $n^2\epsilon_o$ term from contributing significantly. In this case, the Helmholtz energy reduces to

$$F_v = -3NkT^2 \ln \sum_{n=0}^{\infty} e^{-n\hbar\omega/kT} = 3NkT \ln\left(1 - e^{-\hbar\omega/kT}\right) , \tag{14}$$

which is the well-known result from the Einstein model.

The Liquid Potential Function

The zero-degree potential energy in the liquid phase is represented by

$$F_k = \begin{cases} L_1\, e^{2b(1-\xi)} - \dfrac{BV_o}{V} & ; \quad \xi \geq \xi_1 \\ L_o\left(e^{2b(1-\xi/\xi_1)} - 2\, e^{b(1-\xi/\xi_1)}\right) + E_m & ; \quad \xi \leq \xi_1 \end{cases} , \tag{15}$$

where L_1, B, E_m, and ξ_1 are empirical constants peculiar to the liquid phase, and L_o and b are the same as in the solid potential, equation (1). This particular form was chosen for the following reasons.

4. See problem 12 in D. ter Haar, Problems in Quantum Mechanics, Academic Press, New York, 1960. Actually, there should be a 1/2 added to n in both terms corresponding to the ground state. However, the ground state energy is included in the zero-degree lattice terms; therefore, it is suppressed in the vibrational terms.

For $\xi \geq \xi_1$ the repulsive term is the same as in the Morse potential, but the attractive term is the form resulting from van der Waals forces. This potential function cannot be extended to small ξ because eventually the attractive term will override the repulsive term. To avoid this, the form given for $\xi \leq \xi_1$ was chosen. This is identical to the Morse curve for the solid except that E_m and ξ_1 have been introduced to account for the heat of fusion and different compressibility of the liquid phase.

The pressure is again given by $P_k = -(\partial F_k/\partial V)_T$ and is

$$P_k = \begin{cases} \dfrac{2bL_1}{3\xi^2 V_o} e^{2b(1-\xi)} - \dfrac{BV_o}{V^2} \; ; \; \xi \geq \xi_1 \\ \dfrac{2bL_0}{3\xi_1 \xi^2 V_o}\left[e^{2b(1-\xi/\xi_1)} - e^{b(1-\xi/\xi_1)} \right] ; \; \xi \leq \xi_1 \end{cases} \qquad (16)$$

Of the four additional constants introduced in this potential, two are required to match the F_k and P_k at $\xi = \xi_1$. The remaining two are chosen to produce the observed energy and pressure at the melting point[5]. Figure 1 compares the liquid potential with the Morse potential for aluminum.

The Liquid Vibrational Component

The Lennard-Jones Devonshire model of liquid and dense vapors treats each atom as though it were moving in a cage of its nearest neighbors which are considered fixed. Since the number of nearest neighbors is usually 12, a high degree of symmetry exists, and a spherically symmetric potential may be assumed. Following these concepts, the same form of potential function as assumed for the solid, equation (3), is used to describe the behavior of an atom in such a cage.

The partition function will be somewhat different from equation (6), however, because of particle indistinguishability. In the solid phase, particles are, in a sense, distinguishable because of their definite position in the lattice. In a liquid, particles can exchange positions and thereby lose their distinguishability. The partition function must be adjusted accordingly for "proper Boltzmann counting." Since each atom occupies a cell with volume (2a) [3], a volume containing N atoms spaced at average distance, a, can have N/8 cells. There are $(N/8)^N$ ways of arranging N particles among N/8 cells, of which N! are redundant because of particle indistinguishability. The partition function becomes

$$Z = \frac{(N/8)^N}{N!} \, 3N \sum_{n=0}^{\infty} e^{-\epsilon_n/kT} \; . \qquad (17)$$

The Helmholtz energy becomes, using Stirling's approximation,

$$F_v = NkT\,(\ln 8 - 1) - 3NkT \ln \sum_{n=0}^{\infty} e^{-\epsilon_n/kT} \; . \qquad (18)$$

The energy eigenvalues, ϵ_n, are given by equation (5); the internal energy and heat capacity are given by equations (8) and (9), respectively, and the pressure is given by equations (10) and (12), except that the Einstein frequency and the Gruneisen ratio will have different values for the liquid.

It is interesting to examine the behavior of the liquid in the limit of large volumes where $\hbar\omega \to 0$. In this limit, the atom moves freely within its "cage." Encounters with the wall correspond to elastic point collisions characteristic to an ideal gas. Since $kT \gg \epsilon_o$, the summations may be replaced with integrations and

$$\sum_{n=0}^{\infty} e^{-\frac{(n^2+2n)\epsilon_o}{kT}} \to \left(\frac{\pi kT}{4\epsilon_o}\right)^{1/2} \qquad (19)$$

The Helmholtz energy becomes

$$F_v = -NkT - \frac{2}{3} NkT \ln \left[\frac{mkT}{2\pi\hbar^2} \left(\frac{V}{N}\right)^{2/3} \right] . \qquad (20)$$

5. The parameter, ξ_1, is the value of ξ corresponding to minimum potential in the liquid phase. It will generally be more than unity because the distribution of the atoms in liquid metals is random instead of the more efficient close packing usually associated with crystal lattices. This choice of functional dependence was made to assure $P_k(\xi_1) = 0$ and to make the F_k and P_k approach the same values as the solid phase at small ξ.

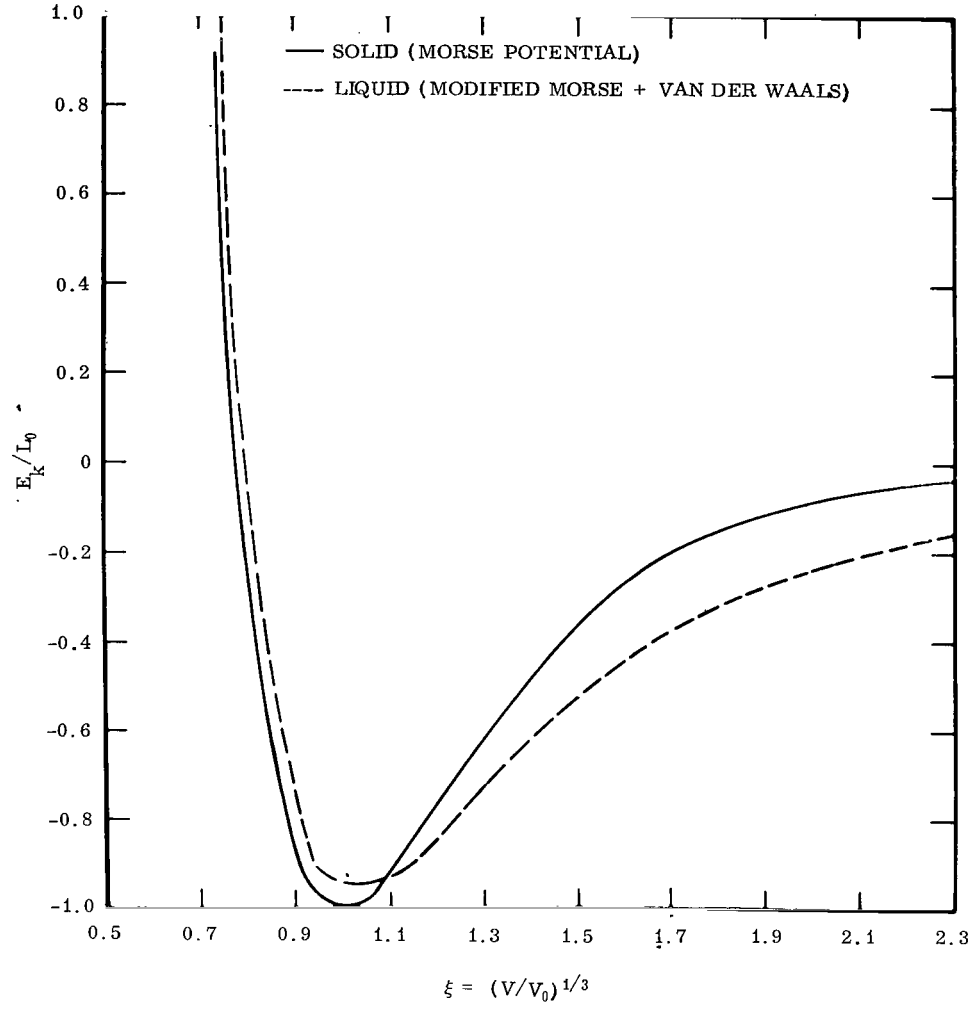

Figure 1. Comparison of solid and liquid potentials. (The liquid potential approaches the solid at high compressions, differs by approximately the heat of fusion at $V = V_o$, and exhibits a van der Waals behavior at large volumes.)

Similarly, the other equations reduce to the ideal gas relations, $E_v = \frac{2}{3} NkT$, $P_v = \frac{NkT}{V}$, and $C_{vv} = \frac{3}{2} Nk$. Using the result of equation (20), the relations $S = (E-F)/T$, and the fact that $E_k = F_k$, the entropy in this limit becomes

$$S = \frac{5}{2} Nk + \frac{3}{2} Nk \ln \left[\frac{mkT}{2\pi\hbar^2} \left(\frac{V}{N} \right)^{2/3} \right], \quad (21)$$

which is the well-known Sakur-Tetrode equation for the entropy of an ideal gas.

At liquid densities, $\hbar\omega >> \epsilon_o$ and the treatment of the vibrational component of liquids at moderate temperature reduces to the Einstein model. However, the Einstein frequency and the Gruneisen ratio will be different in the case of a liquid.

A crude estimate of the vibrational frequency can be made by considering an atom at the origin with an atom at $\pm a$. The change in potential resulting from a displacement x is

$$\Phi(x) = \Phi(a+x) + \Phi(a-x) - 2\Phi(a) \qquad (22)$$

Using only the repulsive term in the Morse Potential, $\Phi(r) = \Phi_o e^{2b(1-r/a_o)}$,

$$\Phi(x) = 2\,\Phi_o e^{2b(1-\xi)}\left[\cosh\left(\frac{2bx}{a_o}\right) - 1\right]. \qquad (23)$$

For small displacements,

$$\Phi(x) \approx 2\,\Phi_o e^{2b(1-\xi)}\,\frac{4b^2x^2}{a_o^2} \quad . \qquad (24)$$

This has the form of a harmonic oscillator potential with a frequency

$$\omega^2 = \frac{4\,\Phi_o b^2}{m\,a_o^2}\,e^{2b(1-\xi)} \qquad (25)$$

from which $\gamma = \frac{1}{3}\,b\,\xi$. The ω as a function of volume can be found from equation (25) and the value of ω_o at $\xi = 1$. This can be obtained from entropy measurements. In the limit of the Einstein model, the entropy becomes

$$S = 3Nk\left(\frac{\hbar\omega/kT}{e^{\hbar\omega/kT}-1}\right) - 3Nk\ln\left(1-e^{-\hbar\omega/kT}\right) - Nk\,(\ln 8 - 1) \quad . \qquad (26)$$

Given S and T, the above expression can be solved for ω.

Figures 2 and 3 show how the vibrational component of heat capacity approaches ideal gas-like behavior in the limit of high temperatures or low densities.

Electronic Contributions

The electronic terms are obtained by treating the free electrons as an ideal Fermi gas. From the grand partition function, one obtains [9]

$$\frac{N}{V} = g\int_0^\infty \frac{\epsilon^{1/2}d\epsilon}{e^{(\epsilon-\mu)kT}} \qquad (27)$$

and

$$E = g\int_0^\infty \frac{\epsilon^{3/2}d\epsilon}{e^{(\epsilon-\mu)/kT}} \quad , \qquad (28)$$

where

$$g = \frac{2^{7/2}\,\pi m^{3/2}}{h^3} \quad .$$

The chemical potential μ must be found for a given volume and temperature by a numerical iterative solution of equation (27), then equation (28) may be integrated to find E. The pressure is obtained from the identity, $PV = \frac{2}{3}\,E$, which holds for Fermi as well as Bose gases. Since, by definition, the chemical potential is the Gibbs energy per atom, $G = N\mu$. Using the identity $G = F + PV$, the electronic contribution to the Helmholtz energy may be found.

For temperatures that are small compared to the Fermi temperature, the integral in equation (27) may be approximated

$$\mu = \epsilon_F - \frac{\pi^2k^2T^2}{12\,\epsilon_F} + \ldots \quad , \qquad (29)$$

and equation (28) becomes

$$E = \frac{3}{5}\,N\,\epsilon_F + \frac{\pi^2}{4}\,\frac{N\,k^2\,T^2}{\epsilon_F} \quad , \qquad (30)$$

where the Fermi energy ϵ_F is

$$\epsilon_F = \frac{h^2}{8m}\left(\frac{3}{\pi}\,\frac{N}{V}\right)^{2/3} \quad . \qquad (31)$$

The first terms in equations (29) and (30) are the zero-degree degeneracy energy. This is already contained in the lattice terms and will therefore be suppressed. The electronic contribution to the Helmholtz energy is

$$F_e = -\frac{\pi^2 N_e k^2 T^2}{\epsilon_F}$$

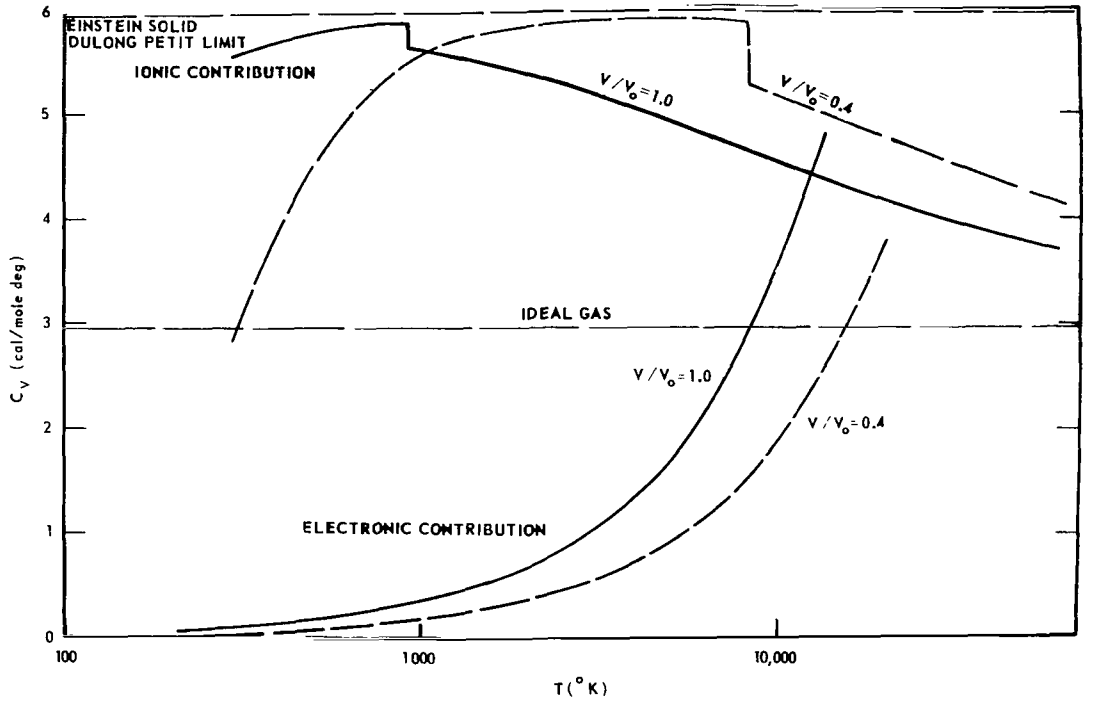

Figure 2. Behavior of heat capacity for solids and liquids in the high temperature regime. (Breaks in the curves represent phase changes.)

The Fermi energy is computed from the observed electronic heat capacity coefficient which can be measured at low temperatures. The C_{ve} is obtained by differentiating equation (30), giving

$$C_{ve} = \left(\frac{\partial E_e}{\partial T}\right)_V = \frac{\pi^2 Nk^2 T}{2\epsilon_F} \quad . \tag{32}$$

At very low temperatures, the electronic terms dominate the heat capacity, which is experimentally observed to depend linearly on T. The value of ϵ_F obtained in this manner will be somewhat different from the value obtained from equation (31) if the free electron mass is used for m. This difference arises from the interaction of the electrons with the lattice. The effective electron mass is defined as that mass which makes equation (31) agree with the Fermi energy obtained from the experimental heat capacity.

COMPUTATIONAL RESULTS

Specification of Constants

The equation of state developed in the preceding section was applied to aluminum. The various constants required are obtained in the following manner.

The zero-degree heat of vaporization L_o is found from tables [10] to be 86 400 kcal/mole. The volume at 0°K is obtained by extrapolation of thermal expansion data and is taken to be 2.736 gm/cm^3. From compressibility data, b is found to be 3.241.

The Slater relation [11],

$\gamma = -\frac{2}{3} - \frac{1}{2} VP_k''/P_k'$, where primes denote

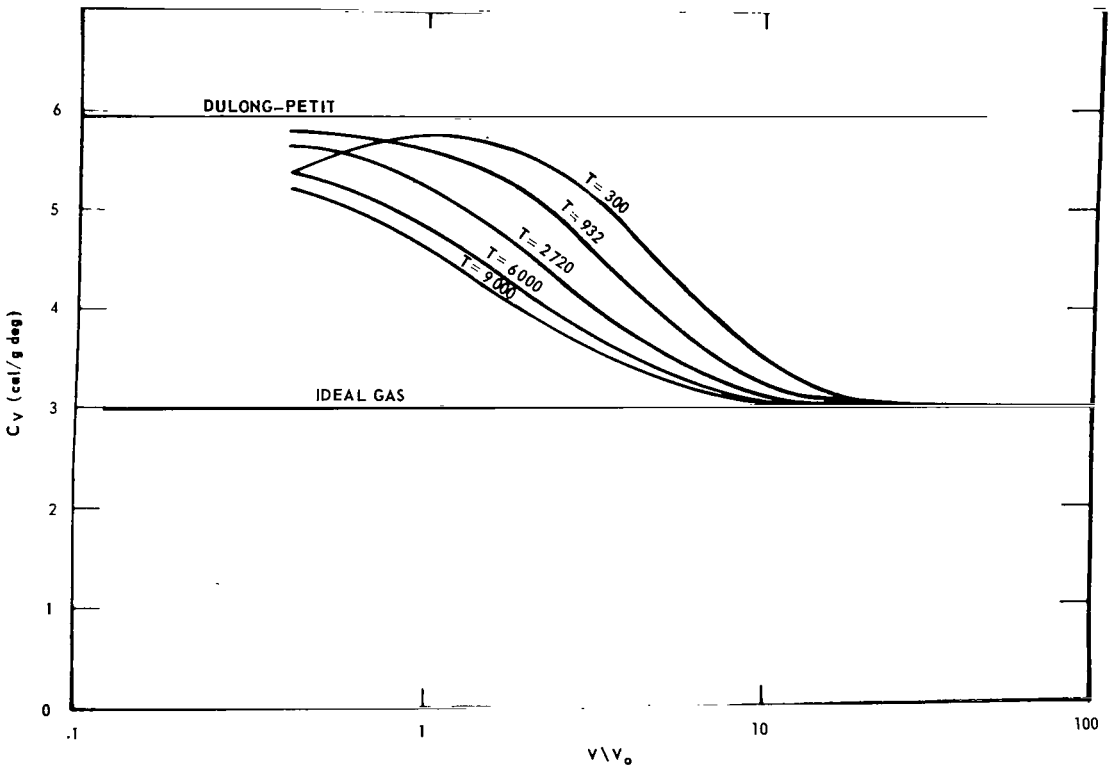

Figure 3. Transition of heat capacity from liquid to gaseous behavior. (The curves indicate the behavior of the vibrational component of the liquid phase only, and ignore the liquid-gas coexistence region.)

differentiation with respect to V, gives γ to within a few percent of the experimental value at normal density. Because of this agreement the Slater relation was used for the calculation for solid aluminum despite the objection that it assumes a volume independent Poisson ratio. In the development of the Slater relation, the result

$$\omega_E^2 = \omega_o^2 \left(\frac{V}{V_o}\right)^{4/3} \frac{P_k'(V)}{P_k'(V_o)}$$

is obtained. Given ω_o, the Einstein frequency at V_o, the ω_E at any other V can be found. The quantity ω_o is found by comparing the entropy of an ideal solid in the Einstein approximation to the measured value at low temperature and using the Slater relation to correct to V_o. For solid aluminum, the Einstein temperature, $\theta = \hbar\omega/k$ was found to be 269.38°K. For the liquid phase, the entropy in equation (26) is used to find the liquid Einstein temperature which is corrected to V_o using equation (25). For liquid aluminum, the Einstein temperature was found to be 117.935°K.

The electronic terms for aluminum are obtained by considering all three valence electrons as free and by taking the effective mass to be 1.6 times the normal electron mass. This brings the calculated electronic heat capacity, equation (32), into agreement with the measured value [12].

The constants L_1, B, E_m, ξ_1 in the liquid potential are found in the following manner. At the melting volume ratio ξ_m and temperature T_m, the

energy is $E_k(\xi_m) + E_v(\xi_m, T_m) + E_e(\xi_m, T_m)$ which must equal to the energy of the zero-degree crystal L_o plus the heat to melt, which is known experimentally. All quantities required to compute $E_v(\xi_m, T_m)$ and $E_e(\xi_m, T_m)$ have been specified; thus, $E_k(\xi_m)$ is known. Similarly, $P_k(\xi_m) + P_v(\xi_m, T_m) + P_e(\xi_m, T_m) = P_{atm}$; therefore, $P_k(\xi_m)$ is known. Using equations (15) and (16) for $\xi \geq \xi_1$, simultaneous equations containing L_1 and B are obtained. Their solution for aluminum yields L_1 = 72 531 cal/mole, and B = 146 397 cal/mole. The quantity ξ_1 is found by requiring the two expressions for P_k, equation (16), to be equal at $\xi = \xi_1$. For aluminum, it was found that $\xi_1 = 1.0265$. Finally, the requirement that both expressions for E_k, equation (18), agree at $\xi = \xi_1$ is used to obtain E_m = 2654 cal/mole.

The Fusion Curve and Equation of State Surfaces

Having specified the various constants for aluminum, computations were carried out for both the solid and liquid phase for various values of ξ and T. Isotherms of a Gibbs energy versus pressure plot are shown in Figure 1. Since the phase that produces the lowest Gibbs energy at a given temperature and pressure is the stable phase, the intersections of the solid-liquid isotherms represent points on the fusion curve (Fig. 5). Using the fusion curve, isotherms are constructed on a P-V surface (Fig. 6), an E-V surface (Fig. 7), and an S-V surface (Fig. 8). Isoenergy lines on a P-V surface are shown in Figure 9.

Comparison with Experimental Results

To compare the equation of state developed in this paper with data obtained from shock compression experiments, the Hugoniot requirement,

$$E - E_o = \frac{1}{2} P(V_{oo} - V) \quad , \qquad (33)$$

is solved simultaneously with the equation of state. In experiments with porous samples, the volume

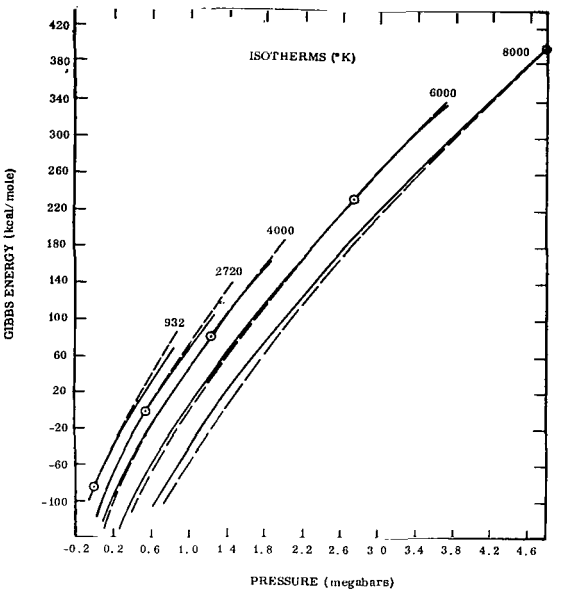

Figure 4. Gibbs energy isotherms. (Circles represent the intersection of the liquid and solid isotherms and determine the melting pressure for that particular temperature.)

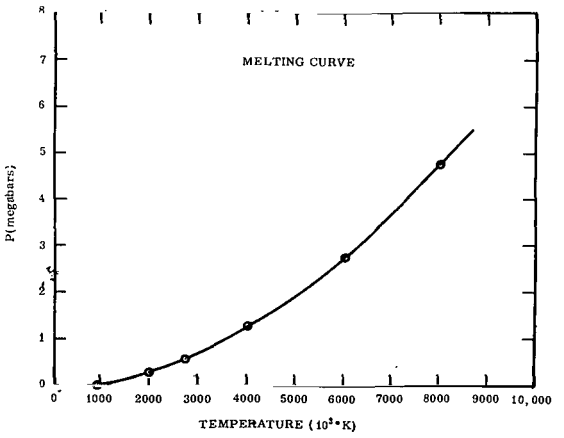

Figure 5. Melting curve deduced from Gibbs energy plot.

V_{oo} represents the actual specific volume of the sample, which may be several times the volume of a

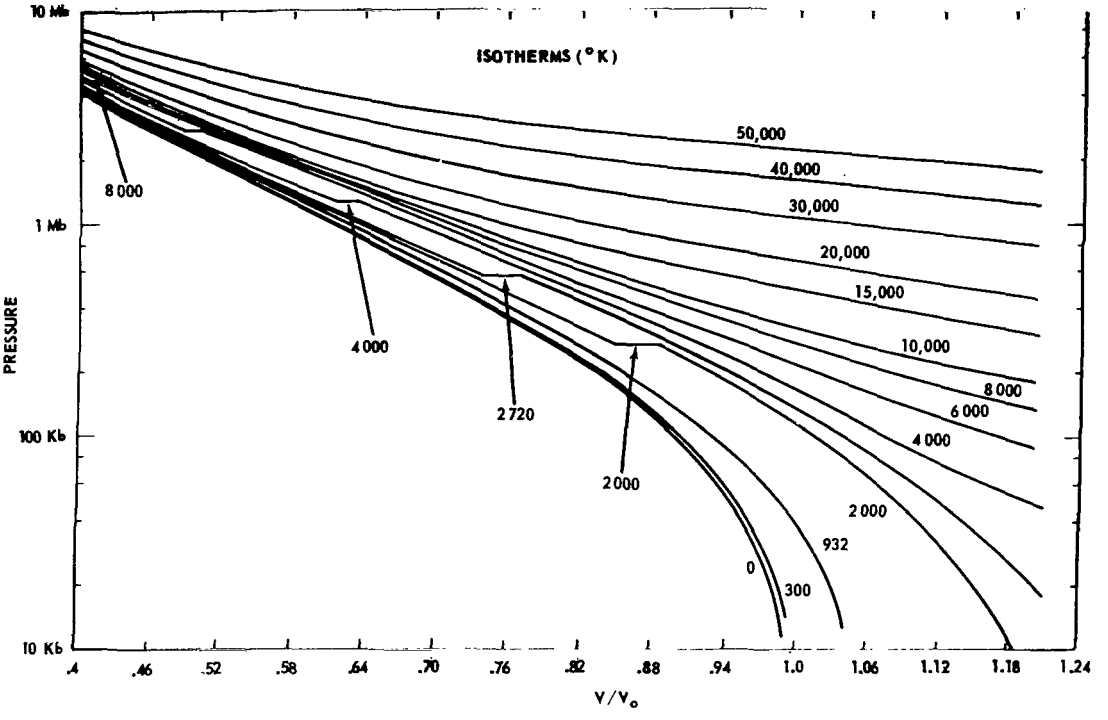

Figure 6. Pressure isotherms. (Breaks in the isotherms represent transition from solid to liquid phase.)

normal crystal. The states that can be reached by shocking a crystal with initial specific volume ratio V_{oo} must lie along the intersection of equation (33) and the equation of state surface in P-V-E space (Fig. 9). By varying the porosity of the sample, any state can, in principle, be reached by shock compression.

In performing shock compression experiments, the observables are the shock velocity D and the material velocity u. These are related to the thermodynamical quantities E, P, and V through the Hugoniot relations

$$V_{oo}(D-u) = VD \quad \text{(conservation of mass)} \quad (34)$$

$$PV_{oo} = Du \quad \text{(conservation of momentum)} \quad (35)$$

These relations are used to relate the observables u and D to the Hugoniot states found by solving equation (33) with the equation of state. Figure 10 compares the predicted results for various porosities with measured results summarized in Table 1. Very good agreement is obtained considering that the equation of state constants are determined solely from ambient properties and contain no constants adjusted to fit the high-pressure data. The highest pressure datum point falls somewhat above the predicted curve for liquid aluminum, but is below the curve for solid aluminum. The fusion curve clearly indicates that melting should have occurred at this state, but the fact that the material was shock compressed may have prevented the phase transition to become complete in the short time involved, and the discrepancy could be that the aluminum is behaving as a super-heated solid. On the other hand, the inaccuracies in the model, particularly in the assumption of a Morse potential configured from the ambient compressibility, could easily account for such a discrepancy at pressures of 5 Mb.

The reproduction of states on the Hugoniot for normal crystal density is not a particularly crucial test for an equation of state. The lattice terms are

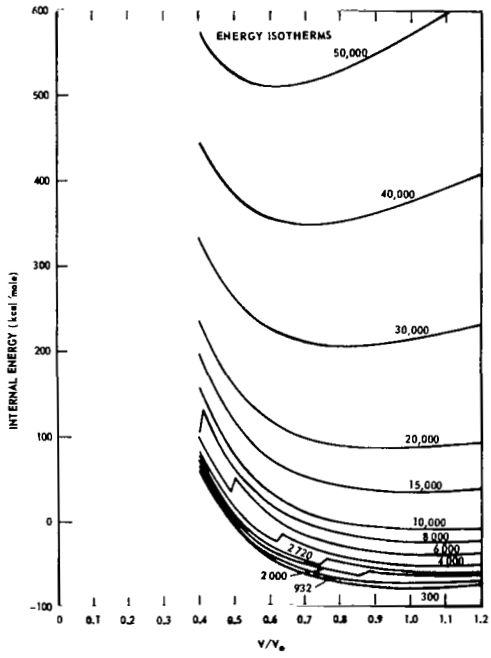

Figure 7. Energy isotherms. (Breaks in the isotherms represent transitions from solid to liquid phase.)

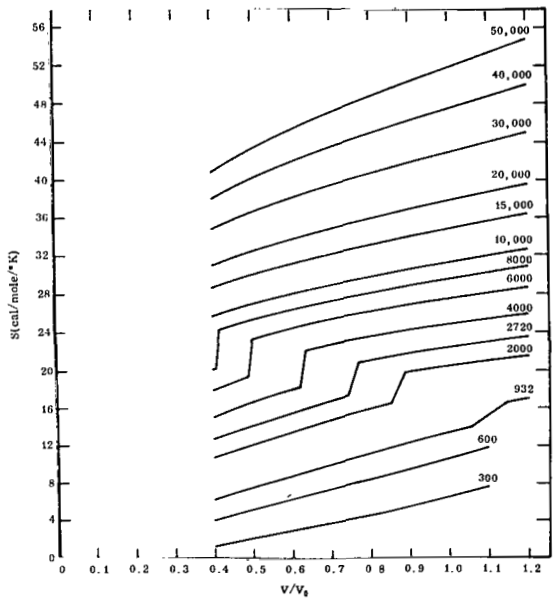

Figure 8. Isotherms on S-V plot. (Breaks in the isotherms represent transitions from solid to liquid phase.)

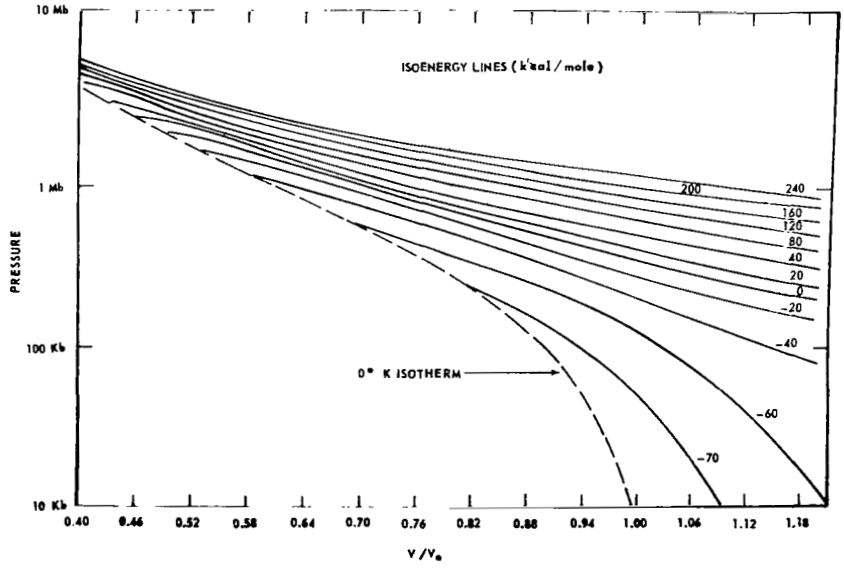

Figure 9. Isoenergy lines. (When lines of constant internal energy are plotted rather than lines of constant temperature, the phase transitions are not apparent.)

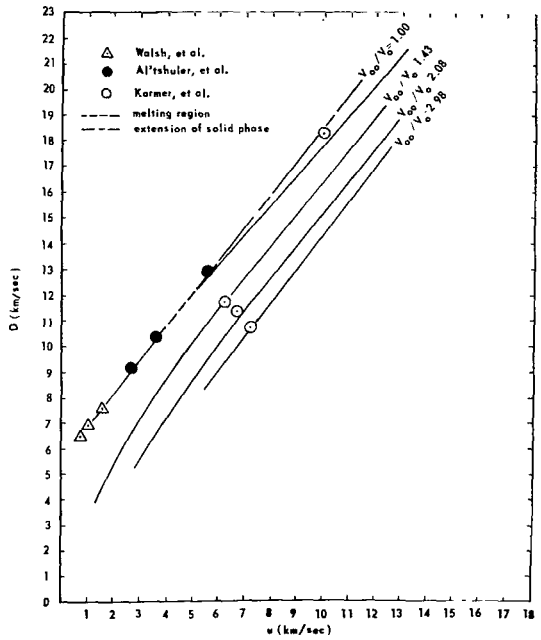

Figure 10. D-u plots comparing computed results with experimental data points. (The short dashed region on the $V_{oo}/V_o = 1$ curve represents the transition region from solid to liquid phase. The long dashed curve represents a superheated solid.)

the major contributors at all but the highest compressions, and the fact that the restoring forces "stiffen up" at high compressions extends the validity of the assumption that the atoms vibrate as harmonic oscillators to high temperatures. Therefore, the Einstein or Debye Model together with the Mie-Gruneisen equation and a properly adjusted zero-degree isotherm will give a good representation of the normal Hugoniot to several megabars. Addition of electronic terms will extend such a model even further. However, such models fail for the lower compression, higher temperature states obtained by shock compressing porous samples. The equation of state developed in this work successfully predicts these states, as shown in Figure 10.

It is useful for shock compression work to plot various thermodynamic coordinates against material velocity u as a means of expressing the thermodynamic state attained in a shock process. The material velocity is particularly useful because it can be easily related to the relative velocity of the impacting samples. Figure 11 is a plot of pressure for different porosities versus u, and experimental points are shown for comparison.

Figure 12 is a plot of temperature in the shocked region as a function of u. The various datum points are illustrated not as a comparison, since measurement of temperatures were not made, but as an indication of the range of temperatures accessible to this technique. The fact that higher temperatures are produced by increasing the porosity is dramatically illustrated by comparing the temperature for the 1.43, 2.08, and 2.98 points and 1.00 point at 5.62 km/sec. These states were created by the same impact velocity. The fact that there is a discontinuity

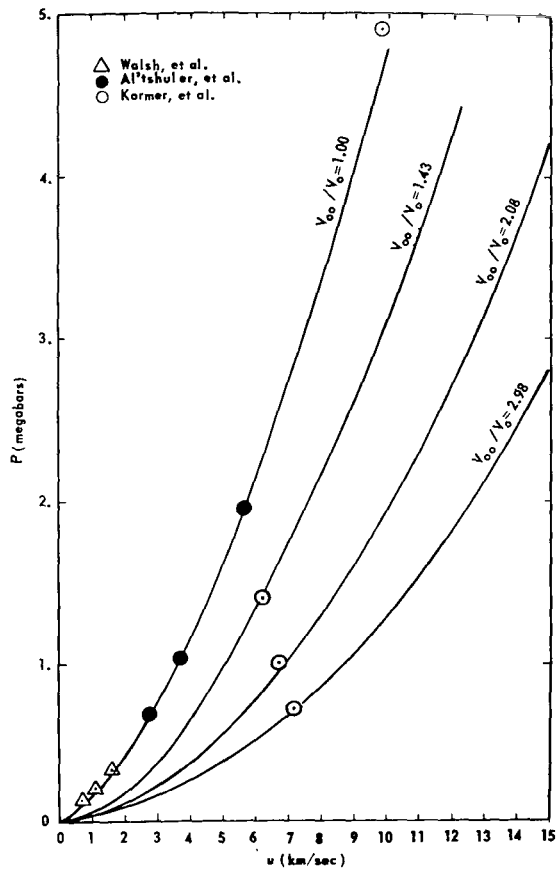

Figure 11. P-u plots comparing computed results with experimental data points. (No abrupt change is apparent that would indicate a phase transition.)

TABLE 1. SUMMARY OF HUGONIOT DATA FOR ALUMINUM

GROUP I[a]			
D (km/sec)	u_f (km/sec)	P(kb)	V/V_o
7.531	3.230	335.8	0.7874
6.927	2.319	222.7	0.8333
6.500	1.700	153.5	0.8696

GROUP II[b]			
D (km/sec)	u (km/sec)	P(kb)	V_o/V
9.13	2.80	693	1.442
10.39	3.70	1042	1.553
12.94	5.62	1971	1.767

GROUP III[c]				
V_{00}/V_{300}	D (km/sec)	P(Mb)	V_o/V	u[d]
1.00	18.31 ± .16	4.93	2.185	9.93
1.43	11.74 ± .10	1.391	1.498	6.25
2.08	11.42 ± .09	1.003	1.176	6.74
2.98	10.75 ± .08	0.702	1.015	7.18

[a] These are representative points of those listed by J. M. Walsh, M. H. Rice, R. G. McQueen, and F. L. Yarger, Phys. Rev.; 108, 196 (1957) The Material velocity u is taken to be 1/2 the measured free surface velocity, u_f.

[b] L. V. Al'tshuler, S. B. Kormer, A. A. Bakanova, and R. F. Trunin; Soviet Physics – JETP, 11, 573 (1962)

[c] S. B. Kormer, A. I. Funtikov, V. D. Urlin, and A. N. Kiksnikova, Soviet Physics – JETP, 15, 477 (1962)

[d] The quantity u was not stated in the paper. It was recovered by the relation $u = [1 - (V/V_o)(V_{300}/V_{oo})]\ D$.

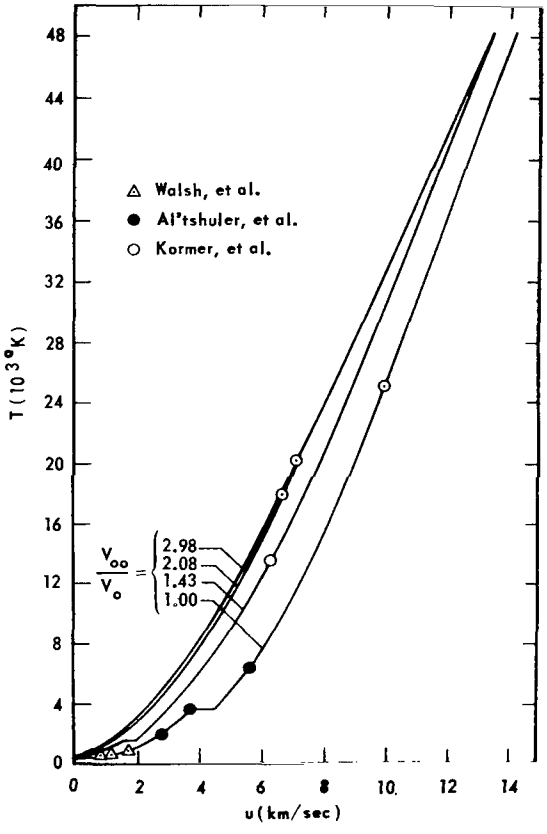

Figure 12. T-u plots. (The data points are shown only to indicate range of temperatures reached by present experimental techniques. The break in the curves indicates that temperature measurement could serve as a method of detecting phase transitions.)

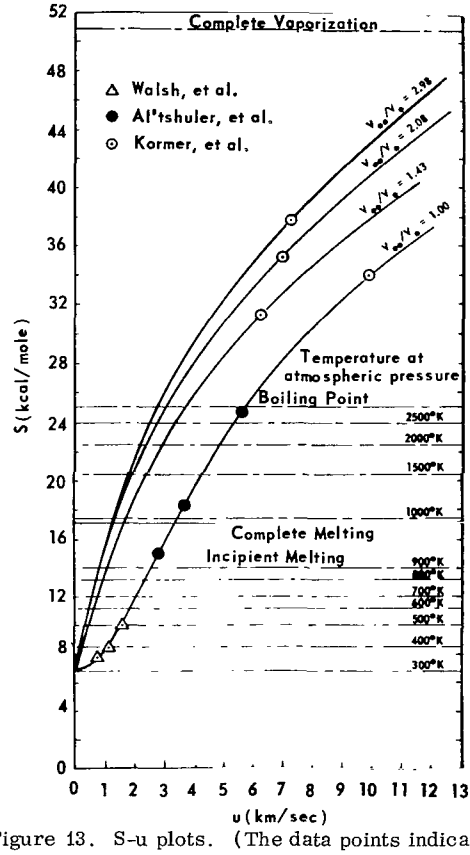

Figure 13. S-u plots. (The data points indicate measurement range rather than actual measurements. The dashed lines indicate entropy values corresponding to the stated temperatures at ambient pressure. If the release is assumed to be isentropic, these can be used to indicate release temperature.)

in the temperature curve at the melting region gives a possibility of experimentally detecting the melting point at very high pressures, although such temperature measurement would be extremely difficult to make in solids.

Figure 13 is a plot of entropy as a function of u. As before, the indicated data points are intended only to indicate range of experimental states, not measurements. For comparison, the temperature and phase of aluminum at ambient pressure for various values of entropy is indicated. Assuming the release is adiabatic and isentropic, an estimate of the release temperature can be made. Attempts have been made to measure the release temperature of shock compressed solids. Taylor [13] reports a favorable comparison between calculated and measured release temperatures for Cu up to the melting point.

CONCLUSIONS

A complete equation of state for metals that describes both the solid and liquid-dense vapor phase has been developed. All empirical constants required can be obtained from elementary thermodynamic data at ambient conditions. Since all thermodynamic functions are derived from the partition function, thermodynamic consistency is guaranteed. Phase transitions between the solid and liquid come about

naturally by using the Gibbs energy to determine the stable phase for a given state. Detailed computations were carried out for aluminum and the ability for the model to predict the behavior of aluminum for pressures of 5 Mb and temperatures of 20 000°K was demonstrated. Since only elementary thermodynamic data at ambient conditions are required to configure the model, extension to other metals is straightforward by insertion of their appropriate constants.

The model can be extended to higher temperatures with some additional computational effort to obtain the electron contributions for temperatures comparable to the Fermi temperature. The model can also be extended to lower densities, provided the temperatures are low enough to completely neglect electronic contributions.

REFERENCES

1. Al'tshuler, L. V.; Bakanova, A. A.; and Trunin, R. F.: JETP, vol. 15, no. 477, 1962.
2. Pastine, D. J.: J. Appl. Phys., vol. 35, no. 3407, 1964.
3. Slater, J. C.: Introduction to Chemical Physics. Chapter XXII, McGraw Hill, New York, 1939.
4. Lennard-Jones, J. E.; and Devonshire, A. F.: Proc. Roy. Soc., London, vol. A163, no. 53, 1937.
5. Pastine, D. J.: Phys. Rev., vol. 166, no. 703, 1968.
6. Liebfried, G.; and Ludwig, W.: Solid State Physics. Vol. 12, Academic Press, New York, 1961.
7. Kormer, S. B.; Urlin, V. D.; and Popova, L. T.: Soviet Physics — Solid State, vol. 3, no. 1547, 1962.
8. Urlin, V. D.: Soviet Physics — JETP, vol. 22, no. 341, 1966.
9. Huang, K.: Statistical Mechanics. Chapter 9, Wiley and Sons, New York, 1963.
10. Stull, D. R.; and Sinke, G. C.: Thermodynamic Properties of the Elements. American Chemical Society, Washington, D. C., 1956.
11. Slater, J. C.: Introduction to Chemical Physics. Chapter XIV, McGraw Hill, New York, 1939.
12. Kittel, C.: Solid State Physics. Chapter 11, Wiley and Sons, New York, 1956.
13. Taylor, J. W.: J. Appl. Phys., vol. 34, no. 2727, 1963.

George C. Marshall Space Flight Center
National Aeronautics and Space Administration
Marshall Space Flight Center, Alabama 35812
124-09-02-00

NASA-Langley, 1970 —— 17 M433

NATIONAL AERONAUTICS AND SPACE ADMINISTRATION
WASHINGTON, D. C. 20546
OFFICIAL BUSINESS

FIRST CLASS MAIL

POSTAGE AND FEES PAID
NATIONAL AERONAUTICS AND
SPACE ADMINISTRATION

01U 001 42 51 3DS 70195 00903
AIR FORCE WEAPONS LABORATORY /WLOL/
KIRTLAND AFB, NEW MEXICO 87117

ATT E. LOU BOWMAN, CHIEF,TECH. LIBRARY

POSTMASTER: If Undeliverable (Section 158 Postal Manual) Do Not Return

"The aeronautical and space activities of the United States shall be conducted so as to contribute . . . to the expansion of human knowledge of phenomena in the atmosphere and space. The Administration shall provide for the widest practicable and appropriate dissemination of information concerning its activities and the results thereof."

—NATIONAL AERONAUTICS AND SPACE ACT OF 1958

NASA SCIENTIFIC AND TECHNICAL PUBLICATIONS

TECHNICAL REPORTS: Scientific and technical information considered important, complete, and a lasting contribution to existing knowledge.

TECHNICAL NOTES: Information less broad in scope but nevertheless of importance as a contribution to existing knowledge.

TECHNICAL MEMORANDUMS: Information receiving limited distribution because of preliminary data, security classification, or other reasons.

CONTRACTOR REPORTS: Scientific and technical information generated under a NASA contract or grant and considered an important contribution to existing knowledge.

TECHNICAL TRANSLATIONS: Information published in a foreign language considered to merit NASA distribution in English.

SPECIAL PUBLICATIONS: Information derived from or of value to NASA activities. Publications include conference proceedings, monographs, data compilations, handbooks, sourcebooks, and special bibliographies.

TECHNOLOGY UTILIZATION PUBLICATIONS: Information on technology used by NASA that may be of particular interest in commercial and other non-aerospace applications. Publications include Tech Briefs, Technology Utilization Reports and Notes, and Technology Surveys.

Details on the availability of these publications may be obtained from:

SCIENTIFIC AND TECHNICAL INFORMATION DIVISION

NATIONAL AERONAUTICS AND SPACE ADMINISTRATION

Washington, D.C. 20546